Mixed Anhydrides: Physical Properties Influenced by Molecular Structure

John H. Penn,*,† Walter H. Owens, Jeffrey L. Petersen,* Harry O. Finklea,* and Daniel A. Snider

Department of Chemistry, West Virginia University, Morgantown, West Virginia 26506

Received September 25, 1992

A series of mixed anhydrides has been prepared and characterized. The reduction potentials and the electronic absorption spectra show an interesting systematic variation which is dependent on the steric requirements of the substituents. X-ray structural results are consistent with theoretical calculations that predict structural variations which are also dependent on the size of the substituent at the anhydride terminus. Taken together, these data show that the relative molecular orbital energies, as influenced by the relative dihedral angle of the two anhydride carbonyl groups, are responsible for the observed changes in physical properties.

Introduction

It has been of particular interest in our department to develop new methodology for the cleavage of specific bonds within molecules.[1,2] A particularly difficult problem for fossil fuel conversion processes has been that of the carboxylic acid functional group since carboxylic acids are unreactive to normal catalytic conditions.[3] The results described here are the consequence of our efforts to convert

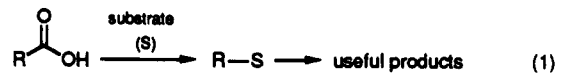

(1)

the carboxylic acid to a more reactive functional group wherein the subsequent reactivity could be easily controlled (eq 1). Although the conversion of carboxylic acids to acyl halides, followed by reduction methodology, is well known,[4] the reaction conditions and byproducts are not very useful for eventual elaboration into process technology.

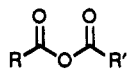

compound	R	R′
1a	Ph	CH_2Ph
2a	Ph	CH_2Ph
2b	4-BrC_6H_5	$CHPh_2$
3a	Ph	CPh_3
3b	4-BrC_6H_5	CPh_3
3c	3,5-$(NO_2)_2C_6H_4$	CPh_3
4	C_6H_{11}	CPh_3
5	Ph	$C(CH_3)_3$

With these constraints in mind, we have prepared a series of mixed anhydrides where the conversion of R–S (see eq 1) might be controlled by the differing bond strengths of the two carbonyl carbon to carbonyl oxygen bonds within the anhydride. An important component of our research strategy was to utilize systematic changes in molecular structure to provide stronger validation of our interpretations. Thus, compounds **1–3** were synthesized to evaluate the relative importance of phenyl substitution with regard to regioselective bond cleavage of the mixed anhydride. A cyclohexyl-substituted mixed anhydride (i.e., **4**) was synthesized to examine dialkyl-substituted anhydrides, while **5** was prepared to compare the stereoelectronic effects arising from trialkyl vs triaryl substitution in these systems.

Although numerous literature references regarding the enormous synthetic utility of anhydrides exist, very limited information is available concerning the reactivity of anhydrides as a function of their structure. Theoretical studies on the structures of simple anhydrides (e.g., acetic anhydride) predict that the compound will adopt an "anti" conformation where the carbonyl groups are oriented 180° apart.[5] Subsequent investigations using spectroscopic methods including dynamic NMR and microwave spectroscopy have verified the accuracy of these theoretical predictions for formic and acetic anhydrides.[6]

The structures of more complex anhydrides are less certain. For example, an attempted X-ray crystal structure determination, as well as IR studies, of benzoic anhydride yielded data from which the syn, the anti, or an intermediate conformation could not be proven as the preferred structure.[7] Because significant changes in reactivity occur upon altering the number of phenyl groups (i.e., **1–3**), we have undertaken a systematic study to evaluate the factors that influence the preferred conformations of anhydrides. Our results are reported here.

Results

Anhydride Synthesis. The anhydride synthesis of Blumberg and MacKellar[8] was modified to prevent difficulties associated with the introduction of water into the system due to hydrate formation and hydrogen ion production. In this modification,[9] an appropriate base is added to the solution to prevent water and hydrogen ion buildup. Our methodology utilized the direct formation of an acyl pyridinium complex (formed from the appropriate acyl chloride and pyridine), which is then treated with the appropriate carboxylic acid as shown in eq 2. All anhydrides utilized in this study were synthesized in this

† Author to whom correspondence should be addressed.

(1) Penn, J. H.; Lin, Z. *J. Am. Chem. Soc.* **1991**, *113*, 1001.
(2) Penn, J. H.; Deng, D.-L.; Aleshire, S. K. *J. Org. Chem.* **1988**, *53*, 3572.
(3) Freihaut, J. D.; Proscia, W. M. *Energy and Fuels*, **1989**, *3*, 625.
(4) Rodina, L. L.; Korobitsyna, I. K. *Russ. Chem. Rev.* **1967**, *36*, 260.
(5) Lee, I.; Cha, O.-J.; Lee, B.-S. *J. Phys. Org. Chem.* **1990**, *3*, 279.
(6) (a) John, I. G.; Radom, L. *J. Mol. Struct.* **1977**, *39*, 281. (b) Vaccani, S.; Bauder, A.; Günthard, H. H. *Chem. Phys. Lett.* **1975**, *35*, 457. (c) Boogaard, A.; Geise, H. J.; Mijlhoff, E. C. *J. Mol. Struct.* **1972**, *13*, 53. (d) Noe, E. A.; Raban, M. *J. Chem. Soc., Chem. Commun.* **1974**, 479.
(7) Collet, H.; Germain, A.; Commeyras, A. *Bull. Soc. Chim. Fr.* **1974**, *2*, 279.
(8) Blumberg, J. H.; MacKellar, D. G. (FMC Corp.) U.S. 3,560,529 (cl. 240–346.8; c 08f), **1968**; 4 pp.
(9) Fife, W. K.; Zhang, Z.-D. *Tetrahedron Lett.* **1986**, *27*, 4933.

0022-3263/93/1958-2128$04.00/0

Table I. Reduction Potential Data

compound	E_r^P (V vs SCE)[c]
benzoyl peroxide	−0.16[b]
3a	−0.95[a]
5	−0.98[a]
4	−1.09[a]
2a	−1.21[a]
phenyl acetate	−1.30[b]
1a	−1.58[a]
benzoic anhydride	−1.62[a,b]
methyl benzoate	−2.32[b]

[a] This work. [b] Reference 9. [c] Estimated uncertainty is ±10 mV.

manner. See the Experimental Section for complete details and characterization data.

(2)

Reduction Potential Data. Peak potentials for the reduction (E_r^P) of anhydrides, **1a–5**, in acetonitrile at 295 K were measured by cyclic voltammetry relative to a sodium-saturated calomel electrode at a voltage sweep rate of 100 mV/s. These data are gathered in Table I.[10] Although E_r^P is not a true thermodynamic quantity (i.e., it is nonreversible), the peak potentials reflect trends in data for related compounds. In addition to the mixed anhydride E_r^P data determined in this work, literature data for related compounds are presented. To ensure that our results were consistent with literature comparisons, we have also determined the E_r^P of benzoic anhydride. These data are also included in Table I.

One result worth noting from this data is that the mixed anhydrides **1a–3a** become much easier to reduce with increasing phenyl substitution. For example, **3a** is 0.63 V easier to reduce than **1a**, while the E_r^P (**2a**) lies at an intermediate value. This is surprising when one considers the fact that the formally nonconjugated di- and triphenylmethyl groups change the peak reduction potential by up to 0.6 V. Confirmation of the facile reduction of these anhydrides is provided by **4** and **5**. The absolute magnitude of E_r^P for **4** may not be directly comparable to **1a–3a** since the replacement of the benzoyl molecular orbital with alkyl substitution would be expected to dramatically change the energy of the LUMO orbital. Compound **5** provides evidence that trialkyl substitution has a similar effect to triaryl substitution. From this electrochemical data, it is apparent that these substituents have a dramatic effect on the ease of reduction for these mixed anhydrides.

Electronic Absorption Spectra. The UV-vis spectra of anhydrides **1a**, **2a**, and **3a** were acquired in benzene and THF. Relevant spectra of anhydrides **1–3** in benzene are shown in Figure 1. To ensure that there was no interference in the absorption spectrum of **3a** due to background absorption by benzene, the reported spectra were carefully checked as a function of the **3a** concentration and the magnitude of ϵ was verified at all reported wavelengths. The origin of each absorption (i.e., n–π^* or π–π^*) was assigned based on the shift of the absorption maxima as a function of solvent polarity. For example, the spectra for **3a** in THF and in benzene show two distinct peaks. A weaker absorption in THF (λ_{max} = 341 nm, ϵ = 1800) undergoes a bathochromic shift to 350 nm in benzene,

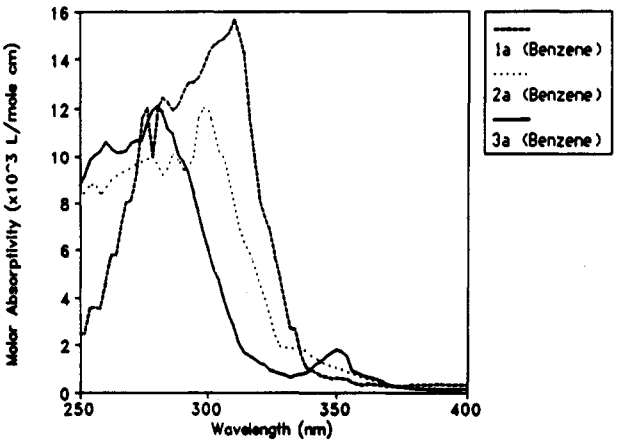

Figure 1. UV-vis spectra for anhydrides **1a**, **2a**, and **3a**.

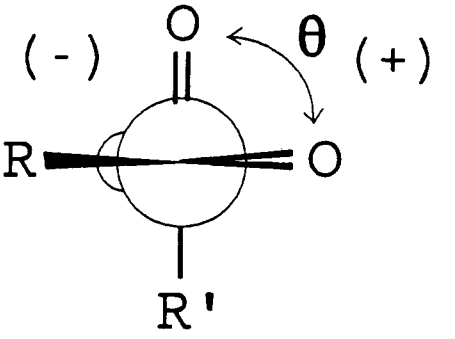

Figure 2. Rotational parameters for a general anhydride structure. This structure is a "Newman-style" projection in which the structure is viewed down the axis of the two carbonyl carbons.

consistent with an assignment of an n–π^* absorption. In contrast, a stronger absorption in THF (λ_{max} = 310, ϵ = 12,000) is hypsochromically shifted to ca. 275 nm in benzene, consistent with an assignment as a π–π^* absorption.

An interesting feature of the data shown in Figure 1 concerns the shifts of each band as a function of the number of phenyl groups in the series **1a–3a**. As the number of phenyl groups is increased across the series, the π–π^* absorption band is systematically shifted to shorter wavelengths. Due to the long wavelength absorption of **1a** and **2a**, it is difficult to determine precisely the position of the n–π^* absorption.

X-ray Structural Data. The structures of anhydrides **2b**, **3b**, and **3c** were determined by X-ray crystallography. Data has been deposited with the Cambridge Crystallographic Data Centre. The coordinates can be obtained, on request, from the Director, CCDC, 12 Union Road, Cambridge, CB2 1EZ, UK. Bromine-containg anhydrides were synthesized to provide the ability to solve the crystal structures by either traditional heavy-atom or direct methods. Complete details of the structure determination are contained within the supplementary material for this paper. The important structural parameter to consider from these studies is the relative orientation of the carbonyl groups as described by Figure 2. In accord with expectations based on steric arguments, these data show that the value of the dihedral angle of **3b** is larger than that of diphenyl **2b** (Table II). Dinitro-substituted **3c** is further twisted than is bromo-substituted **3b**.

Theoretical Predictions of Molecular Properties; Anhydride Structures. For the purposes of discussion, the structure shown in Figure 2 is used to define the angle between the carbonyl groups. Our use of the word

(10) Weinberg, N. L. *Techniques of Electro-Organic Synthesis*; Weissberger, A., Ed.; John Wiley and Sons: New York, 1975.

Table II. Orientation Angles of Carbonyl Groups in Anhydrides as Determined by X-ray Crystallography

compound	R	R′	"dihedral" angle, θ[a]
2b	4-BrPh	$CHPh_2$	31.6 (5)
3b	4-BrPh	CPh_3	42.0 (9)
3c	3,5-$(NO_2)_2$Ph	CPh_3	48.4 (2)

[a] Note Figure 2.

"dihedral" angle to refer to the angles between the planes of the two carbonyl groups stems from defining the dihedral angle to be that of the carbonyl-oxygen to carbonyl-carbon to carbonyl-carbon to carbonyl-oxygen angle. The conformation in which the carbonyl groups are oriented "anti-" to each other corresponds to $\theta = 180°$, while the "syn-" conformation corresponds to $\theta = 0°$. Calculations of the minimum energy conformations were performed by both molecular mechanics (i.e., MMX) and by semiempirical methods (i.e., AM1).[11] By using these contrasting computational methods, trends may be identified, even if the absolute magnitude of the calculated energies cannot be used directly. The results of these calculations are summarized in Table III and have been artibrarily separated into the respective syn- and anti-conformations.

All of the anhydrides in this study showed two local energy minima, one for the syn-conformation and one for the anti-conformation. Several points are noteworthy in these data. First, for most compounds examined here, the anti-conformation is lower in energy than the syn-conformation. For formic anhydride and for acetic anhydride, these results are in agreement with previous theoretical and experimental determinations.[5-7] The preference for the anti-conformation appears to arise from the avoidance of lone pair–lone pair electronic repulsions of the carbonyl groups which are present in the syn-conformation. This assertion is confirmed by calculations of structures in which the electron density in the carbonyl lone pairs is varied by inductive perturbation. The $\Delta\Delta H$ between the anti- and the syn-conformations becomes smaller as electron withdrawing groups are added to one of the anhydride termini. This effect is dramatically accentuated for trichloromethyl 11 where the syn-conformation becomes preferred as chlorine atoms are added to one of the methyl groups of acetic anhydride.

The second noteworthy point of these data concerns the magnitude of θ as the steric requirements of the terminal alkyl groups are increased. The magnitude of θ (note Figure 2) reflects the degree of twisting of the carbonyl groups with respect to each other. Notice that in the optimized syn-conformations, θ increases as the steric requirements of R′ increase. For example, the *tert*-butyl group of **5** and the triphenylmethyl group of **3a** result in predicted minimum energy structures with a high degree of twist (56.2 and 62.3°, respectively). In contrast, **7** is predicted to be planar ($\theta = 1.3°$). A similar trend is noted for the anti-conformations. For the anti-conformations, decreasing θ implies a greater angle of twist. Therefore these calculations are in accord with normal chemical intuition which predicts twisting of the anhydride structure to minimize steric interactions.

A final point concerning these data is the magnitude of the barrier to convert the minimum energy anti-isomer into the minimum energy syn-isomer. To evaluate this effect, the structure of the anti-isomer was selected and used as the basis of a full rotation of the dihedral angle. The dihedral angle was varied in 10° increments while allowing all other parts of the molecule to optimize. The energetics of the rotation are shown in Figure 3. The data depicted in Figure 3 show that the height of the barrier is small, irregardless of whether the syn- or the anti-conformation is the energetically preferred conformation (≤4.1 kcal/mol). These data also indicate that the barrier in going from the high energy isomer to the low energy isomer can be quite small. To confirm that the observed energetics were not affected by the size of the R and R′ groups of the anhydride, the energy barrier for rotation from the anti- to the syn-conformation was also calculated in a similar fashion for **2b** using the AM1 method. The calculated rotational barrier is only 1.3 kcal/mol, in spite of the increased steric requirements of the diphenylmethyl group. Although the exact magnitude of the interconversion barrier contains some uncertainty, the barrier must be sufficiently small that interconversion of the syn- and anti-conformations can occur readily at room temperature in solution conditions where crystallization occurs.

Theoretical Predictions of Molecular Properties; Electronic Effects. Electron affinity data (EA) can be calculated using the AM1 method with reliable results obtained within a given series of closely related compounds.[12] EA is defined in eq 3 as the difference in the

$$EA = \Delta H_f°(RA) - \Delta H_f°(N) \quad (3)$$

heat of formation of the radical anion ($\Delta H_f°(RA)$) and the heat of formation of the neutral species ($\Delta H_f°(N)$).

The calculated EA data are shown in Figure 4 for **7** and **10** as a function of the dihedral angle θ. Similar results have been obtained for **11** but are not shown because these data require a dramatically different scale. The trend is quite clear. The electron affinity of the anhydride increases as the dihedral angle approaches 90°.

The dependence of the EA on the dihedral angle between the carbonyl groups implies that the orbital energies depend on the twist angle. Thus, one may also reasonably expect that changes in the excited state energies or changes in the UV-vis absorption spectra will be observed as a function of θ. For predictive purposes only, the excited state energies were defined simply as the difference in energy between the LUMO and the low level occupied molecular orbitals as calculated by the AM1 method. Close examination of the occupied orbitals reveals two distinct n-orbitals at high energy (n_s and n_a, respectively[13]). The n_s orbital is the HOMO orbital and gives rise to an n_s–π^* excited state when an electron is promoted to the LUMO orbital. Similarly, the n_a orbital is the second highest occupied molecular orbital and gives rise to an n_a–π^* excited state. With these notations in mind, the dependence of the excited state energies are shown in Figure 5. It is readily apparent that dihedral angle changes of the carbonyl groups, whether starting in the syn- or the anti-conformation, result in significant changes in the excited state energies. Most surprising is the direction of change of the excited state energies. The two n–π^* excited states exhibit opposite trends as the carbonyl groups are twisted, with the lowest energy excited state (i.e., the n_s–π^* state) becoming higher in energy when the carbonyl groups are twisted at a 90° angle. Most importantly, the π–π^* excited state becomes higher in energy as θ goes toward 90°. These

(11) Some AM1 calculations could not be performed in our laboratory because of the size restrictions imposed by the initial parameterization.

(12) Dewar, M. J. S., Dennington, R. D., II. *J. Am. Chem. Soc.* **1989**, *111*, 3804.

(13) Orchin, M.; Jaffé, H. H. *Symmetry, Orbitals, and Spectra (S.O.S.)*; Wiley-Interscience, John Wiley and Sons, Inc.: New York, 1971; p 309.

Table III. Calculated Minimum Energy Geometries for Anhydrides (all energies in kcal/mol)

			anti-conformation			syn-conformation		
compound	R	R'	θ	ΔH_f (MMX)	ΔH_f (AM1)	θ	ΔH_f (MMX)	ΔH_f (AM1)
6	Ph	H	178.9	-74.1	-98.9	-1.1	-71.0	-95.9
7	H	H	177.4	-87.4	-121.3	-1.3	-86.6	-120.5
8	H	CH_3	176.2	-93.8	-123.5	-3.6	-89.9	-119.5
9	Ph	CH_3	176.1	-90.7	-102.5	-4.2	-86.9	-98.9
10	CH_3	CH_3	172.6	-95.7	-121.9	-6.4	-93.2	-118.5
11	CCL_3	CH_3	162.1	-97.6	-129.4	-19.2	-100.0	-130.9
1a	Ph	CH_2Ph	161.6	-52.9	-66.6	-19.1	-49.1	-62.7
2a	Ph	$CHPh_2$	149.4	-49.6	-58.4	-30.9	-47.7	-56.5
2b	4-BrC_6H_5	$CHPh_2$	138.8	-50.7	-61.8	-33.5	-49.4	-60.4
4	C_6H_{11}	CPh_3	124.5	-56.3	-	-39.8	-54.1	-
5	Ph	$C(CH_3)_3$	123.8	-69.2	-84.3	-56.2	-66.7	-81.9
3a	Ph	CPh_3	117.7	-43.2	-	-62.3	-41.9	-
3c	$(NO_2)_2C_6H_4$	CPh_3	-106.7	-21.7	-	+46.4	-19.9	-
3b	4-BrC_6H_5	CPh_3	103.4	-31.2	-	-43.3	-29.0	-

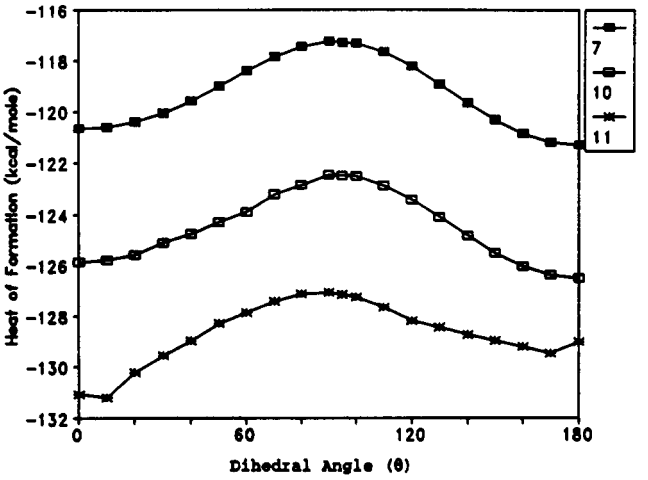

Figure 3. Heat of formation dependence (AM1) upon orientation of the carbonyl groups.

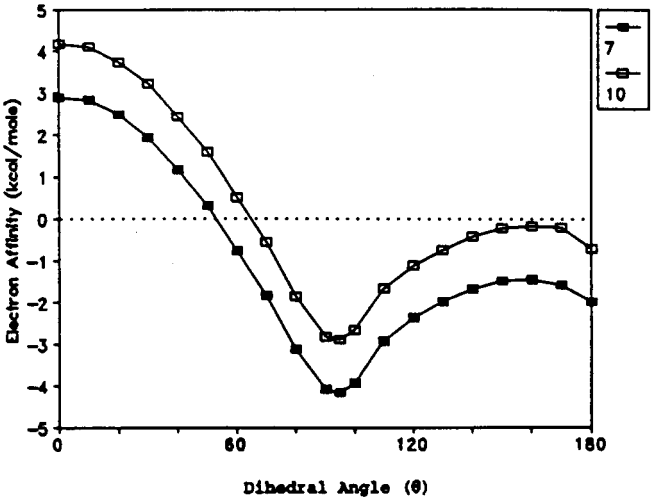

Figure 4. Electron affinity dependence upon the orientation of the carbonyl groups for formic anhydride (7) and acetic anhydride (10).

changes in excited state energies should be observable as changes in transition energies.

Discussion

Structure of Mixed Anhydrides as a Function of Substitution. The results of our efforts to predict molecular structures through the use of theoretical methods have been summarized in Table III. Anhydrides with relatively small substituents were seen to prefer the syn- or the anti-conformation of the carbonyl groups. As the

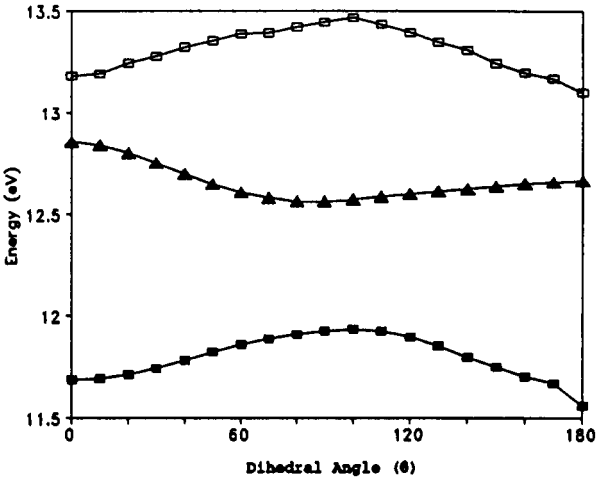

Figure 5. Calculated electronic absorption data for 7. (□) π–π^*, (▲) n_a–π^*, (■) n_s–π^*.

size of the substituents increase the carbonyl groups are predicted to be twisted to an increasing extent with respect to each other. This steric effect is most readily demonstrated in the series of compounds **9**, **1a**, **2a**, and **3a** in which phenyl groups are added systematically to one side of the anhydride. Using the MMX method the preferred dihedral angles increase systematically (i.e., 3.9°, 18.4°, 30.6°, and 62.3°) in this series of compounds. The AM1 calculated minimum energy geometries are similar. These results imply that the gas phase structure becomes more twisted as the steric demands of the substituents increase.

The critical question for this study is whether the calculated structures approximate the solution phase structure. For this purpose, X-ray crystal structures were obtained for **2b**, **3b**, and **3c**. As noted previously, all structures crystallize in the syn-conformation with an increasing twist angle of the carbonyl groups as the size of the substituent on the anhydride becomes larger. For example, **2b** shows calculated and experimentally determined dihedral angles of 33.5 and 31.6° respectively, **3b** shows values of 43.3 and 42.0°, respectively, and **3c** shows values of 46.4 and 48.4°, respectively. While the agreement is not exact, it is well known that force field calculations have difficulty in properly evaluating the relative effects of steric repulsion and resonance interactions in predicting exact conformations.[14] Alternatively, crystal lattice packing forces may be responsible for the slight differences.

(14) Hohlneicher, G.; Penn, J. H.; Müller, M.; Demmer, M.; Lex, J.; Gan, L.-X.; Loesel, P. D. *J. Am. Chem. Soc.* **1988**, *110*, and the references therein.

(15) Williams, A. E.; Lee, J. K.; Schowen, L. R. *J. Org. Chem.* **1973**, *38*, 4053.

We believe that increasing twist angle exhibited by the X-ray structure determinations verify the predictions of steric interactions in these molecules. The twisting of the molecule in the gas phase (as predicted computationally) becomes greater as the steric interactions increase. The X-ray results are complementary in that the twist angle becomes larger as steric interactions are increased. From these results, one would expect the structure of the mixed anhydrides in solution to be similar to that predicted in the gas phase in the absence of extensive interactions of solvent molecules with the solute molecules.

Although the agreement of the calculated structure with the experimentally determined structure is quite good, the preference for the syn-conformation is somewhat surprising in light of the experimentally determined anti-conformation for **7** and **10** and the calculated lower energy anti-conformations for these mixed anhydrides. Two alternative rationales may explain this behavior. Crystal lattice packing forces may be responsible for the observed preference for the syn-conformation. The difference in energy between the syn- and the anti-conformations is always small regardless of the substituents R and R'. At most, the anti-conformation is calculated to be more stable than the syn-conformation by ≤3 kcal/mol. Further, the enthalpy barrier to rotation from the syn- to the anti-conformation is surprisingly low. As seen in Figure 3, the $\Delta\Delta H$ for rotation from the syn- to the anti-conformation of several anhydrides is ≤4 kcal/mol. These energy differences are all accessible at room temperature as the crystals are formed from the solution for the purposes of an X-ray structure determination. With these slight energy differences between the syn- and anti-conformations, crystal lattice packing forces could be responsible for the observed preference. An alternative rationale for the preference for the syn-conformation may be the electron withdrawing groups which were placed on **2b**, **3b**, and **3c**. The anti-conformation is predicted to be the preferred conformation for **7** and **10**, presumably because of electron-electron repulsion of the lone pair electrons in the syn-conformation. However, inductive removal of electron density (e.g., **11**) is shown to make the syn-conformation more accessible. Underestimation of the removal of electron density by the computational method may cause a sufficient change in the preferred conformation as to tip the balance to give the wrong prediction.

Although the energetically preferred conformation of the anhydrides may not be completely understood, the twisting of the carbonyl groups with increasing size of the substituents is clear. Whether the conformation of **3** is syn or anti, molecular mechanics, AM1, and the X-ray structural analyses show clearly the trend toward increasing twist in the series **1**, **2**, and **3**. The increasing twist is responsible for the changes in physical properties in these anhydrides as noted below.

Reduction Potential Measurements. The increased twist of **3** relative to **2** and **1** is likely to be responsible for the dramatic decrease in the E_r^P. The theoretical dependence of the EA is shown in Figure 4. Although the syn-conformation shows a high EA (i.e., less easy to reduce), a minimum EA is calculated at a dihedral angle of 90°. In the series **1**, **2**, and **3**, where increasing twist has been confirmed, the E_r^P mirrors the calculated and the observed change in the dihedral angle for the carbonyl groups. For example, the calculated optimal angle for the series **1**, **2**, and **3** (161.6°, 149.4°, and 117.7°) is reflected by the change in E_r^P for the same series (−1.58, −1.21, and −0.95 V vs SCE). The dependence of the E_r^P on the dihedral angle of the carbonyl groups is supported by data for **5** (E_r^P = −0.98 V) in which the *tert*-butyl group is expected to provide similar steric effects and, therefore, a significant amount of twist (calculated twist angle =123.8°). The data for **4** are not directly comparable since the cyclohexyl and triphenylmethyl substituents provide a dialkyl anhydride as compared to an arylalkyl anhydride (e.g., **1**, **2**, **3**, **5**). However, the low value for the E_r^P (−1.09 V) makes it very tempting to speculate that a significant twist in this compound leads to an easier reduction.

An alternative explanation of the reduction potential data involves the interplay of the competing effects of the shift in the reduction potential caused by the irreversibility of the chemical reactions following electron transfer and the shift in the reduction potential caused by the potentially heterogeneous electron transfer at the electrode surface. One might use a Curtin-Hammett type of argument in which facile conformer change leads to a species which is more easily reduced or undergoes more rapid followup reactions as we examine the trends exhibited in this series of compounds. Rapid followup reactions create an artificial situation where the compounds appear to be reduced more easily than would be otherwise expected. We exclude this argument for two reasons. First, although a low barrier to rotation is expected, the fully syn- (θ = 0°) and the fully anti-conformations (θ = 180°) of compounds **3a**, **5**, and **4** are high-energy conformations as shown by the theoretical and X-ray studies. Conformational change from the syn- to the anti-conformation likely occurs through the low-energy 90° conformation. The molecule does not spend any significant amount of time in the planar conformations. Second, **3a** and **5** are exceptionally easy to reduce and might be expected to undergo rapid bond cleavage of the just-formed radical anions because of the stability of the radical and anion fragments to be formed. However, cyclohexyl **4** has a reduction potential which is less negative than **2a**. Cyclohexyl **4** has no relatively easy bond cleavage pathways of the radical anion being envisionable while **2a** would be expected to yield highly stabilized products and therefore react rapidly. The effects of heterogeneous electron transfer work in the opposite direction. In this series of compounds, it is the most sterically hindered compounds that yield the lowest reduction potentials. This is opposite to the expectations based on normal considerations of heterogeneous electron transfer. Thus, while we cannot definitively rule out an explanation in which the reduction potentials are influenced by a Curtin-Hammett consideration, we believe that twisted anhydrides show a lower reduction potential based only on the twist angle.

Effects of Twisting on UV-vis Absorption Spectra. As noted earlier, the excited state energies are also affected by the angle of twist of the carbonyl groups (Figure 5). From a theoretical standpoint, both the π–π^* and the n_s–π^* excited states are at higher energy when the carbonyl groups are twisted, relative to either the syn- or the anti-conformations. As indicated earlier, the λ_{max} of the π–π^* absorption shows a systematic shift to higher energy in the series **1**, **2**, and **3** (Figure 1). Although not shown, the absorption spectrum of **5** is similar to that of **3**, confirming the high degree of twist for the π–π^* absorption spectrum.

The effect of twisting on the n–π^* absorption is less certain. Although the n–π^* absorption band is clearly visible for **3**, we were unable to conclusively identify the

n–π* absorption band for 1 and 2. Efforts to increase the concentration of these compounds or efforts to identify the position of either n–π* absorption by solvent shifts of the peak maxima were fruitless.

Summary

A number of mixed anhydrides have been synthesized. A comparison of theoretical and solid-state X-ray structural data indicates that the dihedral angle between the carbonyl groups increases as the size of the substituents increase. This twisting produces significant changes in the reduction potential and the UV-vis absorption spectra of these compounds.

Experimental Section

Melting points were determined on a Laboratory Devices Meltemp apparatus and are uncorrected. Gas-liquid chromatographic analyses were conducted on a Hewlett-Packard Model 5890A GLC equipped with a 10-m 5% phenylmethylsilicone or a Carbowax 20M Megabore column. HPLC was performed on a Waters Associates Protein Peptides I system capable of gradient elution and using UV detection at 254 nm. Integration of the signals was performed by a Hewlett-Packard Model 3390A digital integrator. GCMS were measured with a Hewlett-Packard Model 5980 mass spectrometer with a 5890 gas chromatograph equipped with a 25-m 5% phenylmethylsilicone column. IR spectra were recorded on a Midac Model or a Perkin-Elmer Model 1310 FTIR spectrophotometer. ^{1}H NMR spectra (δ (ppm) and J (Hz)) were measured in the indicated solvent with TMS as an internal standard on a JEOL-GX-270 NMR spectrometer. UV-vis spectra were measured with a DMS-100 spectrophotometer. X-ray structural data were acquired with a Picker full-circle goniostat under computer control from a Krisel Control diffractometer automation system. Geometries of structures were calculated using the PCMODEL program (Version 3.1, 1987) on an IBM 386 PC computer and the AM1 program (MOPAC version 3) on a VAX 8650. Cyclic voltammetry data were acquired with a BAS CV-27 potentiostat and a Houston Instruments recorder. Low-resolution mass spectra were obtained on a Hewlett-Packard 5980 spectrometer and high-resolution mass spectra on a CEC DuPont 21-110B spectrometer.

Benzene was dried by distillation from $LiAlH_4$. Pyridine was dried by distillation from KOH. Acetonitrile was predried by distillation from CaH_2 followed by distillation from P_2O_5 and then K_2CO_3. Benzoic acid, triphenylacetic acid, cyclohexanecarboxylic acid, *p*-bromotoluene, 3,5-dinitrobenzoyl chloride, benzoyl chloride, phenylacetic acid, phenylacetyl chloride, phenylacetic acid, tetraethyl ammonium perchlorate, and cyclohexanecarbonyl chloride are available from Aldrich Chemical Co. and were used without further purification. Diphenylacetyl chloride (available from Aldrich Chemical Co.) was recrystallized from $CHCl_3$ prior to usage. Anhydrides 1[15] and 5[8] have been previously reported although compound 1 has not been fully characterized in the literature.

Anhydride Synthesis. A typical preparation procedure follows. The acyl chloride (6.9 mmol) was added to a solution of 20 mL of previously dried benzene and dry pyridine (7.0 mmol) under nitrogen. Stirring was continued until a finely divided white precipitate was observed which indicated the formation of the reactive acyl halide–pyridinium complex. The reaction vessel was placed in an ice bath at −10 °C and the carboxylic acid was added all at once. The temperature of the solution initially increased by ca. 15 °C, but returned to a lower temperature after stirring for an additional 20 min at −10 °C. The reaction mixture was filtered through Celite on a glass frit. The solvent was then removed in vacuo to yield product which was purified as indicated below.

Benzoic phenylacetic anhydride (1a): 89.6% yield; mp 61–63 °C (hexane/benzene); ^{1}H NMR δ 7.31–7.45 (m, 10 H), 6.22 (s, 2 H); ^{13}C NMR δ 49.2 (benzylic), 127.4 (arom), 128.2 (arom), 128.4 (arom), 128.5 (arom), 128.8 (arom), 129.2 (arom), 133.1 (arom), 138.5 (arom), 162.1 (CO), 168.2 (CO); FTIR (CCl_4) ν (cm^{-1}) 1814.3, 1744.8; GCMS m/z 240 (P, 27%), 77 (76%), 105 (100%), 119 (37%), 91 (56%); UV-vis (benzene) λ_{max} 310 nm (ϵ = 15700); high-resolution MS (calcd for $C_{15}H_{12}O_3$, 240.0742) 240.0739.

Benzoic diphenylacetic anhydride (2a): 97.1% yield; mp 144–146 °C (10% ethyl acetate/hexane); ^{1}H NMR δ 7.33–7.41 (m, 15 H), 5.27 (s, 1 H); ^{13}C NMR δ 58.0 (benzylic), 127.7 (arom), 128.5 (arom), 128.6 (arom), 128.7 (arom), 128.8 (arom), 128.9 (arom), 134.4 (arom), 137.2 (arom), 161.8 (CO), 167.8 (CO); FTIR (CCl_4) ν cm^{-1} 1809.1, 1742.8; GCMS m/z 316 (P, 31%), 77 (82%), 105 (100%), 195 (57%), 155 (25%); UV-vis (benzene) λ_{max} 298 nm (ϵ = 12,000); high-resolution MS (calcd for $C_{21}H_{16}O_3$, 316.0979) 316.0981.

4-Bromobenzoic diphenylacetic anhydride (2b). 4-Bromotoluene was oxidized with Na_2CrO_4/H_2SO_4 to yield quantitatively 4-bromobenzoic acid which was reacted in the previous fashion with diphenylacetyl chloride: 94.3% yield; mp 162–163 °C (hexane); ^{1}H NMR δ 5.31 (s, 1 H), 7.35 (m, 10 H), 7.89 (dd, 4 H, J = 42.4 Hz); ^{13}C NMR δ 57.3 (benzylic) 126.5 (arom), 127.1 (arom), 127.4 (arom), 127.8 (arom), 128.1 (arom), 134.2 (arom), 137.5 (arom), 137.8 (arom), 162.1 (CO), 168.4 (CO); FTIR (CCl_4) ν cm^{-1} 1809.5, 1743.1; GCMS m/z 395 (P, 28%), 397 (17%), 77 (56%), 184 (100%), 186 (43%), 195 (35%), 155 (27%); high-resolution MS (calcd for $C_{21}H_{15}O_3Br$, 395.1536) 395.1533.

Benzoic triphenylacetic anhydride (3a): 95.6% yield; mp, 156–157.8 °C (hexane); ^{1}H NMR δ 7.28–7.37 (m, 20 H); ^{13}C NMR δ 68.2 (benzylic), 127.2 (arom), 128.1 (arom), 128.2 (arom), 128.6 (arom), 130.0 (arom), 130.4 (arom), 134.3 (arom), 141.7 (arom), 161.6 (CO), 168.4 (CO); FTIR (CCl_4) ν cm^{-1} 1803.7, 1740.5; GCMS m/z 392 (P, 26%), 77 (73%), 243 (55%), 271 (36%), 105 (100%); UV-vis (benzene) λ_1 349 nm (ϵ = 1800), λ_2 282 nm (ϵ = 12100); high-resolution MS (calcd for $C_{27}H_{20}O_3$, 392.1219) 392.1218.

4-Bromobenzoic triphenylacetic anhydride (3b). 4-Bromobenzoic acid was reacted in the solid phase with PCl_5 in an oil bath maintained at 70 °C. The resulting yellow liquid was evaporated in vacuo to afford 4-bromobenzoyl chloride, a clear, colorless liquid that solidified on cooling. The acid chloride was immediately reacted with triphenylacetic acid in the usual manner to prepare the mixed anhydride: 97.1% yield; mp 173–174 °C (hexane); ^{1}H NMR δ 7.38 (m, 15 H), 7.81 (dd, J = 51.3 Hz 4 H); ^{13}C NMR δ 68.4 (benzylic), 125.6 (arom), 126.3 (arom), 127.4 (arom), 127.8 (arom), 128.9 (arom), 134.2 (arom), 137.6 (arom), 138.1 (arom), 161.5 (CO), 169.2 (CO); FTIR (CCl_4) ν cm^{-1} 1804.1, 1740.1; GCMS m/z 473 (16%), 471 (P, 29%), 77 (65%), 243 (59%), 271 (32%), 184 (100%), 186 (52%); high-resolution MS (calcd for $C_{27}H_{19}O_3Br$, 471.2498) 471.2495.

3,5-Dinitrobenzoic triphenylacetic anhydride (3c): 91.3% yield, mp 182–183 °C (30% ethyl acetic/hexane); ^{1}H NMR δ 7.38–7.43 (m, 15 H), 8.68 (s, 2 H), 9.17 (s, 1 H); ^{13}C NMR δ 67.5 (benzylic), 123.3 (arom), 127.7 (arom), 128.3 (arom), 128.4 (arom), 129.8 (arom), 132.3 (arom), 140.9 (arom), 148.7 (CNO_2), 159.7 (CO), 167.9 (CO); FTIR (CCl_4) ν cm^{-1} 1802.9, 1741.0; GCMS m/z 482 (P, 26%), 271 (34%), 243 (54%), 195 (100%), 77 (61%); high-resolution MS (calcd for $C_{27}H_{18}N_2O_7$, 482.1162) 482.1157.

Cyclohexanecarboxylic triphenylacetic anhydride (4): 94.2% yield; mp 106–108 °C (petroleum ether); ^{1}H NMR in acetone δ 7.29–7.31 (m, 15 H), 2.29 (quintet, J = 5.4 Hz 1 H), 1.54–1.59 (s, 10 H); ^{13}C NMR δ 68.1 (benzylic), 56.4 (cyclohexyl), 15.1 (cyclohexyl), 23.8 (cyclohexyl), 34.9 (cyclohexyl), 126.3 (arom), 127.1 (arom), 128.9 (arom), 133.2 (arom), 164.2 (CO), 168.9 (CO); FTIR (CCl_4) ν cm^{-1} 1811.8, 1742.3; GCMS m/z 398 (P, 31%), 271 (29%), 243 (53%), 111 (100%), 77 (78%); high-resolution MS (calcd for $C_{27}H_{26}O_3$, 398.1695) 398.1693.

Reduction Potential Measurements. A three-compartment cell was charged with the anhydride (10 mM) and recrystallized Et_4NClO_4 (0.10 M) in freshly distilled HPLC grade acetonitrile. The solution was sparged with argon for a minimum of 15 min. A sodium-saturated calomel electrode was employed as a reference with a polycrystalline gold flag (area = 1 cm^2) as the working electrode. The data were collected at a sweep rate of 100 mV/s.

Supplementary Material Available: Tables of crystallographic data, positional parameters, temperature factors, and interatomic distances and bond angles, perspective views of **2b**, **3b**, and **3c**, and ^{1}H NMR spectra of **2a,b**, **3a–c**, and **4** (24 pages). This material is contained in libraries on microfiche, immediately follows this article in the microfilm version of the journal, and can be ordered from the ACS; see any current masthead page for ordering information.